

Photonic Multiple Beam Forming Systems for Broadband RF Antenna Arrays

K. H. Wagner, F. Schlottau, M. Colice, G. Kriehn and R. T. Weverka

Optoelectronic Computing Systems Center, University of Colorado, Boulder, CO 80309-0525
303-492-4661 kelvin@optics.colorado.edu http://optics.colorado.edu/MURI

Abstract: Two broadband, sparse array imaging systems are presented. Both show squint free, true-time delay beamforming capability, but are based on radically different technologies - optical coherent transients and temporally-shaped femtosecond pulses.

1. Introduction

The formation of multiple RF beams pointed toward every far-field source illuminating a large, broadband antenna array is a demanding task which is required for applications in active radar receivers, as well as passive surveillance or communications receivers, and radio-astronomy.¹ These large antenna arrays provide increased sensitivity by coherently combining the RF signals from N individual array elements to point high gain, narrow angular-resolution beams. If the resolvable signal propagation time ($T = L/c$) across the array aperture, L , exceeds the inverse bandwidth of the system, B^{-1} , then true-time-delay (TTD) beam steering is required (with total available differential delay $T = L/c$ approaching 30-300 ns for 10-100 m diameter arrays near end fire). Alternatively, spectrally-selective processing with resolution of at least $\Delta f = c/L = 3 - 30$ MHz can be used to compensate for the aperture scaling and resulting frequency-dependent beam steering (beam squint). At each of $M = BT$ resolvable frequencies, multiple simultaneous beams must be formed in all directions, since the angles-of-arrival of the signals are unknown. In addition, each source within the observable hemisphere can emit over bandwidths that span as much as 10:1 frequency ratios (say 2-20 GHz).

Long antenna baselines, L , provide high angular resolution, $\Delta\theta = \lambda_{\text{rf}}/L$; but fully populating such a large array with antennas spaced at $\lambda_{\text{rf}}/2$ may be prohibitively expensive, and it is difficult to avoid deleterious mutual coupling effects. Instead, sparse, non-redundant arrays can be used. Such irregularly-spaced arrays will have a reduced sensitivity compared to that achievable with a fully-populated aperture, but can achieve extremely high angular resolution with neither grating lobes nor close-in side lobes.¹

Wideband single-beam formation for linear equi-spaced RF antenna arrays is a demanding task that requires a time-delay ramp to be imposed across the array of signals, yielding $s_n(t - nd \sin \theta/c)$, which exactly cancels the delays due to the propagation geometry. Numerous optical approaches to TTD beam forming have been developed utilizing fiber delay lines including fiber grating wavelength tunable delay ramps,²

and even fiber-based multiple beam formers.³ Multiple simultaneous beam formation requires that different time-delay ramps be imposed across the array of antenna-element signals, which are then summed to form the different beams. The frequency domain formulation of a multiple, TTD beam-formation system first temporally Fourier transforms each antenna-element signal with a spectral resolution better than $1/T$, and then each resolvable spectral channel is treated as a narrow-band beam former, allowing simple spatial Fourier transformation using a Fourier kernel that scales with frequency in order to counteract beam squint. Finally, at each beam position, an inverse temporal Fourier transformation is required to recover the time-domain signals.

Narrow-band, multiple-beam forming for a 2-D (planar) RF antenna array can be accomplished optically by placing an array of modulators fed by the corresponding RF antenna elements in a miniaturized topology corresponding precisely to a scaled version of the antenna array and spatially Fourier transforming with a lens.⁴ This approach works for fully-populated RF arrays driving corresponding optical modulators or for sparse, irregularly-spaced arrays in any planar topology. The scaling of the antenna (where elements are typically spaced on the order of $d = \lambda_{\text{rf}}/2$) to the optical modulators (spaced by $D = 100\lambda_{\text{opt}}$), and the simultaneous scaling of the RF wavelength, λ_{rf} to the optical wavelength, λ , scales the full hemisphere of RF angles to about 1 degree of optical angular spectrum. On the other hand, broadband beam forming of these 2-D antenna arrays is substantially more difficult, and to our knowledge, no optical approach that can form all TTD beams for large, ultrabroadband, antenna arrays in real time besides our imaging spectrum analyzer⁵ has been introduced. In this paper, we present two optical TTD, multiple-beam forming systems to produce squint-free, broadband, high-gain beams in every resolvable direction simultaneously.

2. Broadband array signals

Consider far-field RF sources emitting waveforms $f_s(t)$, each arriving with a angle-of-arrival (AOA) unit direction \hat{d}_s , that produce a total field at the array aperture

$$\mathcal{E}(\vec{r}, t) = \sum_s f_s \left(t - \hat{d}_s \cdot \vec{r}/c \right).$$

This field will be detected by the antenna-array elements and will produce signals that need to be delayed

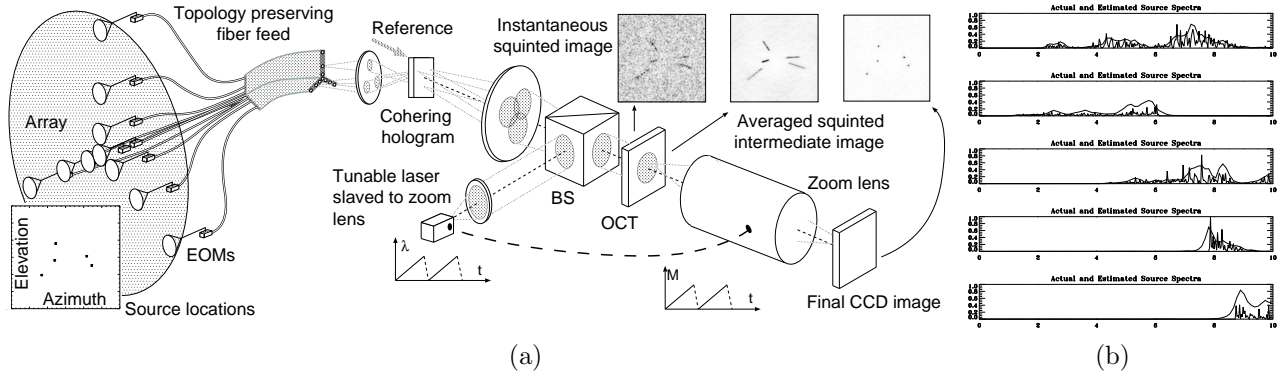


Figure 1: a) Sparse-array correlation imager using a coherently-modulated, fiber-remoted RF antenna array cohered with a photorefractive hologram and then spatially Fourier transformed with a lens onto a spatial-spectral holographic (SSH) medium. The time-integrated, spectrally-selective hologram is read out with a scanned, tunable laser using a variable magnification zoom lens whose magnification is proportional to the laser frequency offset. b) Simulated operation of the SSH array imager showing the estimated time-domain spectra of the sources compared to the actual spectra.

and combined to separate them into their various components. A planar array of N broadband antenna elements at locations \vec{r}_n in the $z = 0$ plane senses the field over an aperture $a(\vec{r}) = \sum_n^N \delta(\vec{r} - \vec{r}_n)$. The N received signals

$$s_n(t) = \mathcal{E}(\vec{r}_n, t) = \sum_s \int F_s(\Omega) e^{i\Omega(t - \hat{d}_s \cdot \vec{r}_n/c)} d\Omega + cc,$$

are amplified and applied to the optical modulators. The modulated optical signals are then propagated through a coherent, topology preserving, fiber-feed network and launched as an array of Gaussian beams, $g(\vec{x})$, from an aperture that duplicates the planar array topology with a magnification m (a 10-100 m diameter RF antenna array might be mapped to a 1 cm fiber feed, giving $m = 10^{-3} - 10^{-4}$).

3. SSH Array Imaging Spectrometer

VanCittert-Zernike theorem based approaches require a cross-correlation of every antenna signal with every other signal to produce a frequency dependent complex coefficient of the scene component in (\vec{k}_T, ω) -space determined by the element separation and frequency (where \vec{k}_T and ω are the transverse spatial and temporal frequency components). After integration of the correlation coefficients for a long time, spatial Fourier transformation of the samples in (\vec{k}_T, ω) -space at each frequency forms a monochromatic RF image which can be detected, while different frequency-component images are scaled proportional to their RF frequency and then summed. Alternatively, the approach from filled-aperture imaging is much more computationally demanding since the spatial Fourier transformation of the RF antenna element signals must be performed at a rate of at least twice the antenna bandwidth, and then mod squared and time-integrated to form the image. In both cases, beam squint is manifested as an image scale factor proportional to the RF frequency, which must be compensated by a frequency dependent scale factor. Our first solution to

this demanding application (see Fig.1) uses a fiber-fed, coherent, optically-modulated array using an electro-optic modulator at every element, phase cohered with a photorefractive crystal.⁶ The cohered output is spatially Fourier transformed onto a thin cryogenically-cooled spatial-spectral holographic (SSH) crystal,⁷ in which each pair of antennas interferes and accumulates a spatial-spectral grating at each resolvable frequency bin of 100KHz (corresponding to a coherence time $T_2 = 10\mu s$) with a \vec{k}_g -vector proportional to the antenna element (and corresponding scaled fiber) separation. After accumulating for about $T_B = 10ms$ (the bottleneck lifetime), a frequency-scanned, plane-wave readout laser diffracts off these gratings in a thin hologram geometry, and is imaged onto a 2-D CCD detector array. As the frequency of the laser is scanned, the system magnification is synchronously varied using a motorized zoom lens over a range corresponding to the bandwidth ratio of the maximum to minimum RF frequencies. Each RF source is localized and simultaneously spectrally analyzed with a wide-open unity probability of intercept array of spectral radiometers which are scanned out in slow time at a convenient rate, orders of magnitude slower than the RF signals, allowing high dynamic range detection. Time integration of these multi-frequency images on the CCD followed by further digital accumulation can produce extraordinarily high DR images after a few seconds, or time varying RF images at video rates.

4. Spectrally multiplexed beamformer

Our second system requires that a high-frequency, piezo-electric transducer be deposited on the core region of an angle cleaved polarization-maintaining, single-mode optical fiber in order to launch multi-GHz acoustic waves into the fiber core. When broadband, spectrally uniform light illuminates the fiber, and an RF signal of frequency f_0 is applied to the transducer (launching an exponentially-decaying acoustic wave) then the optical frequency component that meets the

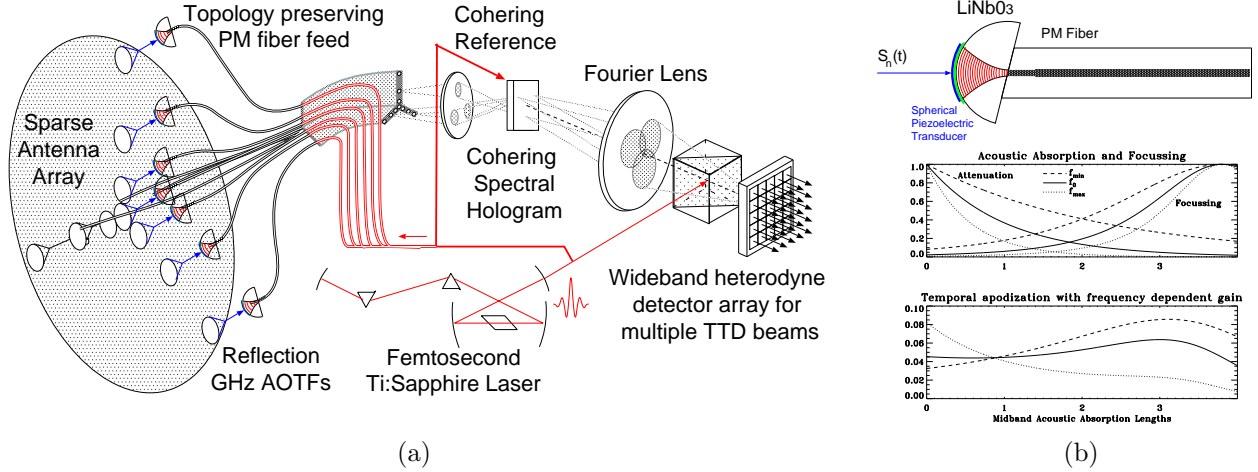


Figure 2: a) Fiber-remoted, sparse antenna array that uses an octave-spanning, femtosecond laser source and multi-GHz, reflective, acousto-optic tuneable-filter modulators at each antenna element. Multiple TTD beam forming is accomplished using a simple Fourier lens where the wavelength variation of the scale factor provides the necessary compensation of beam squint, and heterodyne detection reproduces each antenna beam on a wideband detector array. b) Fiber-optic, acousto-optic tuneable filter for femtosecond pulse shaping of the RF signals from each antenna element. By using a focusing acoustic wave in a low acoustic attenuation crystal, the achievable time delay can be increased to more than 100 ns. The resulting apodizing window functions are illustrated at different frequencies, showing compensation of the attenuation with focusing.

phase matching condition $2\pi f_0/v_A = |\vec{K}_A| = |\vec{k}_x + \vec{k}_y| = 2\pi(n_x + n_y)\nu_0/c$, will be retroreflected, polarization switched, and Doppler shifted, producing an all-fiber, acousto-optic tunable filter (AOTF). The required RF frequency $f_0 = \nu_0(n_x + n_y)v_A/c \approx 8$ GHz for $\lambda = 1.5 \mu\text{m}$ and varies between 6-12 GHz for octave-bandwidth optical illumination in the 1-2 μm region. At these frequencies, exponential acoustic attenuation is extreme since it varies with frequency as $\alpha = \alpha_0 f^2$ (where α_0 is about 7 dB/ $\mu\text{s}/\text{GHz}^2$ for glass), which leads to a number of resolvable spectral channels, $TB = 3/2\alpha_0 f_0$ that can only be as high as 40. This would allow for TTD processing for arrays up to 40×40 elements. Cryogenically cooling the fiber can increase the number of spectral channels to nearly 100 by decreasing the attenuation. Alternatively, coupling into another material for the acousto-optic interaction (such as LiNbO₃ or GaAs), can dramatically increase the acousto-optic efficiency for shear-wave, polarization-switching diffraction, and allow more favorable geometries at the expense of a more complex modulator device structure. For example, LiNbO₃ will have a much lower acoustic attenuation (0.1-1 dB/ $\mu\text{s}/\text{GHz}^2$), and a hemispherical acoustic-wave transducer focusing in the direction opposite to the modal expansion from the fiber can partially compensate for the residual attenuation. This increases the allowable TB by a factor of 3-6, as illustrated in Fig. 2b. When a repetitive train of femtosecond laser pulses with broad, nearly octave-spanning spectra is utilized for readout of the reflection grating, then the reflected light can be considered to be an ultrafast pulse shaper that speeds up the recent history of the RF waveform by a ratio $r = c/n_g 2v_A$, of half the optical group ve-

locity, $v_g = c/n_g$, to the acoustic velocity, v_A . This codes about 10-100 ns of RF history in a 0.2-2 ps shaped optical pulse. For an octave-bandwidth signal, $s(t)$, applied to the piezo-electric transducer, the launched acoustic wave is given by

$$A(z, t) = H(z) \int S(\Omega) e^{i\Omega(t-z/v_A)} e^{-\alpha_0 \Omega^2 z} b(\Omega, z) d\Omega \\ \approx s(t - z/v_A) e^{-\alpha_0 \Omega_0^2 z} H(z) b(\Omega_0, z) = s(t - z/v_A) W(z)$$

with $H(z)$ is a Heavyside step function, $b(\Omega, z)$ represents the amplitude variation due to acoustic focusing, and $W(z)$ represents the center frequency window function. The readout by a counter-propagating femtosecond laser pulse, $\vec{p}(t) = \hat{x} \text{sech}(t/\tau_p) e^{i\omega t}$, produces a polarization-switched diffracted output from the fiber

$$E(t) = \hat{y} \eta s(rt) W(tv_g) * p(t - \tau)$$

with efficiency η , and where τ represents the delay to the fiber output.

To build a squint-free array beam former, we place a fiber-based, high-frequency AOTF at each antenna-array element and interrogate them in parallel with a repetitive pulse train of octave-spanning femtosecond pulses, $\sum_q p(t - qT)$. At each element, the signal is modulated onto the broadband optical spectrum of the reflected shaped pulse. These modulated optical pulses contain the array-element time histories with an exponential weighting. Using the external LiNbO₃ focusing AOTF geometry will allow nearly 300 ns of time delay in an efficient polarization switching interaction. These reflected pulses can also be viewed as containing the RF frequencies coded onto optical wavelengths with an RF resolution of 3 MHz across the 8-16 GHz frequency band, and corresponding optical resolution of about 1 nm in the 1-2 μm

window, or at correspondingly higher RF frequencies (16-32 GHz) in the visible spanning wavelength range (0.5-1 μm). This optical comb of frequencies (spaced at the laser repetition frequency) is spectrally filtered and Doppler-shifted by each applied RF frequency, and allows for a complete, coherent reconstruction of the RF signals by heterodyne mixing of the RF spectral components and low-pass filtering on the detector. The optical field distribution for the q th pulse emerges from the topology preserving fiber feed as a function of transverse position $\vec{x} = (x, y)$,

$$E(t, \vec{x}) = \sum_n \delta(\vec{x} - m\vec{r}_n) * g(\vec{x}) \left[\hat{x}p(t - \tau_n - qT) + \eta\hat{y}s_n(rt) W(tv_g) * p(t - \tau_n - qT) + cc \right],$$

where τ_n represents the length of the n th fiber at a scaled position $\vec{x} = m\vec{r}_n$, with Gaussian profile $g(\vec{x})$. The unmodulated, retroreflected, femtosecond pulse also emerges from the polarization maintaining fiber as an \hat{x} -polarized pulse, and this can be used to record a spectral hologram by interfering it with a slightly delayed, plane-wave reference femtosecond pulse $p(t - \tau' - qT)$, so that the diffraction of the modulated \hat{y} -polarized signals will be both phase and time cohered. Such a spectral hologram could be implemented using an imaging spectrometer geometry in which each fiber is dispersed into a short rainbow on a photorefractive crystal where it is interfered with the reference pulse, and then the cohered diffraction is recombined with a conjugate dispersive element. Alternatively, an intrinsically spectrally selective spatial-spectral holographic material can be used by recording an image plane hologram for fiber array cohering. The emerging modulated component diffracted by the cohering hologram, and passed through a \hat{y} -analyzer, is given by

$$E(t, \vec{x}) = \sum_{n,q} \delta(\vec{x} - m\vec{r}_n) * g(\vec{x}) \eta\hat{y}s_n(rt) W(tv_g) * p(t - \tau' - qT).$$

This field can be Fourier transformed by an apochromatic lens, in which the intrinsic wavelength-dependent, Fourier-plane scale factor $\vec{u} = \vec{x}'/\lambda F$ is exactly the scaling necessary to compensate for RF beam squint, giving

$$E(t, \vec{x}') = \eta\hat{y}G(\vec{u}') \sum_{s,q} \int F_s(\Omega) * w\left(\frac{\Omega}{v_a}\right) p(\Omega r) e^{i\Omega r(\tau' - qT)} A \left[\frac{\Omega r}{2\pi c} \left(\vec{D}_s + m \frac{\vec{x}'}{F} \frac{2n_g}{n_x + n_y} \right) \right] d\Omega$$

where $\vec{D}_s = \hat{d}_s - (\hat{z} \cdot \hat{d}_s)\hat{z}$ is the transverse component of the AOA unit vector, and $A(\vec{u}) = \sum_n e^{-2\pi\vec{u} \cdot \vec{r}_n}$ is the FT of the array aperture. Squint is eliminated since the shift of the argument of A is independent of Ω (slight shifts due to AOTF dispersion may still occur), although the aperture resolution does scale with frequency. This field can be heterodyne detected at each squint-free beam position by adding a reference pulse train to reproduce each broadband signal since the Doppler shifts of each AOTF filtered component contain the coherent RF information.

5. Conclusion

Two new schemes for all-angle, multiple, true-time-delay beam formers for large, 2-D, planar, RF array antennas with the RF signals modulated onto optical beams in a miniaturized antenna topology and then using optical Fourier transformation have been proposed. One approach uses cryogenically-cooled spatial spectral holography to simultaneously record the power spectra of all resolvable far-field RF sources within the field of view of the antenna array. The SSH is then read out with a scanned laser, while a synchronously scanned zoom lens eliminates beam squint by eliminating the frequency dependent scale factor. The second approach shapes the RF signals from each antenna element as femtosecond pulses using fiber AOTFs, and then uses the wavelength-dependent Fourier-plane scale factor of a conventional lens to produce squint-free beams, which can operate up to about an octave of bandwidth. These systems extend the capabilities of previous optical TTD beam formers to large, possibly irregularly spaced, 2-D antenna arrays that form all beams simultaneously, thereby allowing wide-area, high-gain, unity probability-of-intercept, broad-bandwidth, RF array receivers for surveillance, radar, and communication applications.

We wish to gratefully acknowledge the support by Dr. B. Schneider of DARPA AOSP (NRO000-02-C-0629), and Dr. W. Miceli of ONR and the OSD through the DDR&E MURI program (N00014-97-1-1006).

References

- [1] A. R. Thompson et al, *Interferometry and synthesis in radio astronomy*, Wiley, 1986.
- [2] L. J. Lembo et al, "Low-loss fiber optic time delay element for phased-array antennas," in *Proc. SPIE, vol 2155*, 1994, p. 13.
- [3] P J Matthews et al, "A wide-band fiberoptic true-time-steered array receiver capable of multiple independent simultaneous beams," *IEEE PTL*, vol. 10, pp. 722, 1998.
- [4] D.I. Voskresenskii et al, *Electrooptical Arrays*, Springer-Verlag, 1989.
- [5] K.H. Wagner et al, "Array imaging using spatial-spectral holography," in *2002 Optics in Computing*, Taipei, 2002, ICO.
- [6] Robert T. Weverka, Kelvin Wagner, and Anthony Sarto, "3-dimensional holographic data processing and wavelength readout for range-doppler-angle radar and synthetic aperture radar," 1994, vol. 2155, SPIE.
- [7] M Mitsunaga and R G Brewer, "Generalized perturbation-theory of coherent optical-emission," *PRA*, vol. 32, pp. 1605, 1985.